Supplementary information

Computational investigation reveals that the mutant strains of SARS-CoV2 have differential structural and binding properties

Rakesh Kumar[#], Rahul Kumar[#], Harsh Goel and Pranay Tanwar[*]

Dr.B.R.A.-Institute Rotary Cancer Hospital, All India Institute of Medical Sciences, New Delhi, INDIA-110029

***Corresponding author:**

Dr. Pranay Tanwar
Dr.B.R.A.-Institute Rotary Cancer Hospital,
All India Institute of Medical Sciences, New Delhi, INDIA-110029
E-mail: pranaytanwar@gmail.com

[#]**Equal contribution**

Total supplementary figures : 11

Total supplementary tables : 8

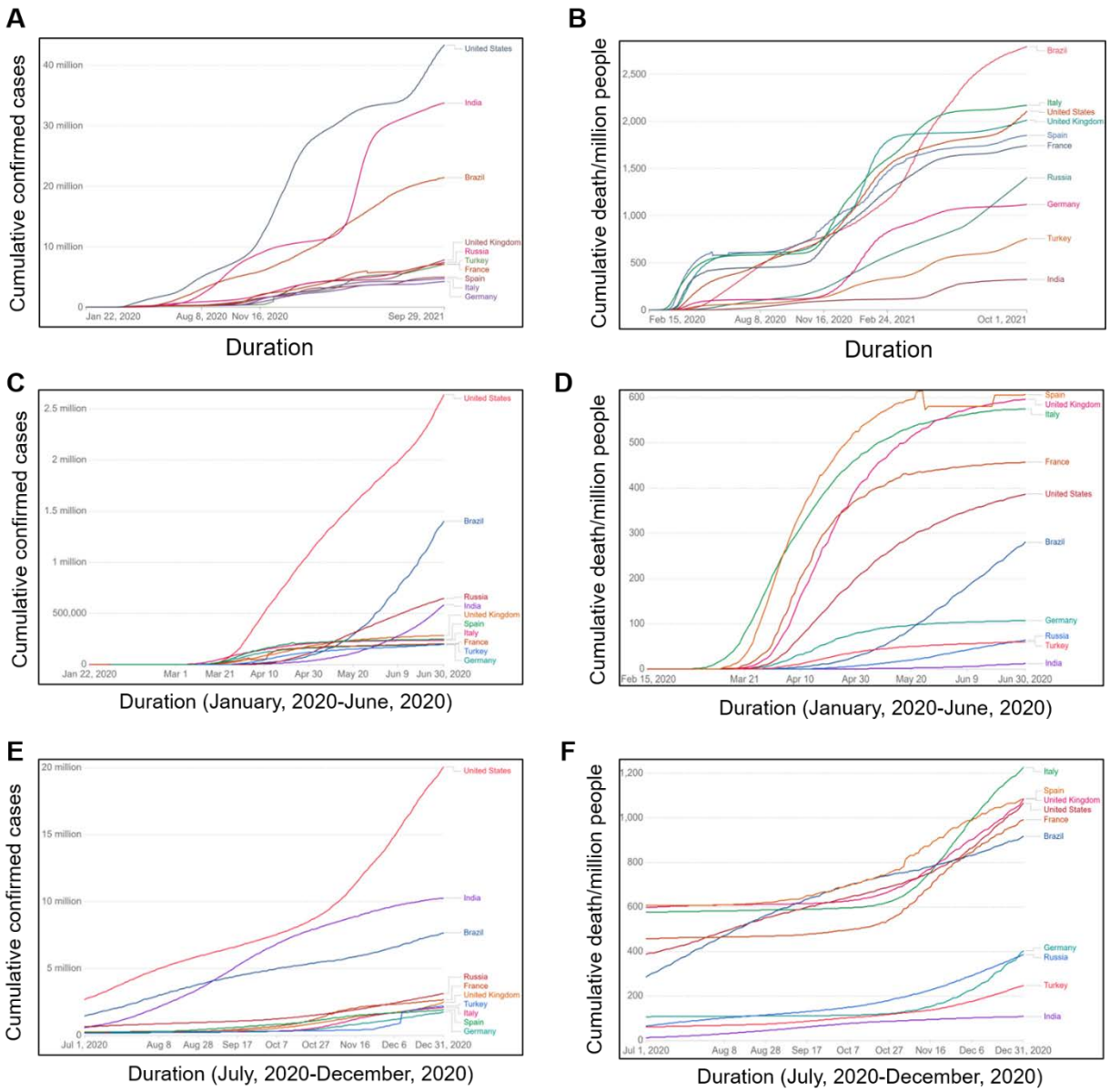

Fig. S1 **Coronavirus pandemic country profile** (till February, 2021)**.** (A) Total conformed cases, (B) Total death/million people, (C) Total confirmed cases of first wave (January, 2020- June, 2020), (D) Total death/million people in first wave, (E) Total confirmed cases of second wave (July, 2020- December, 2020) and (F) Total death/million people in second wave. Different countries were labelled in different colour lines. Data was taken from Coronavirus Pandemic (COVID-19) database. (https://ourworldindata.org/coronavirus).

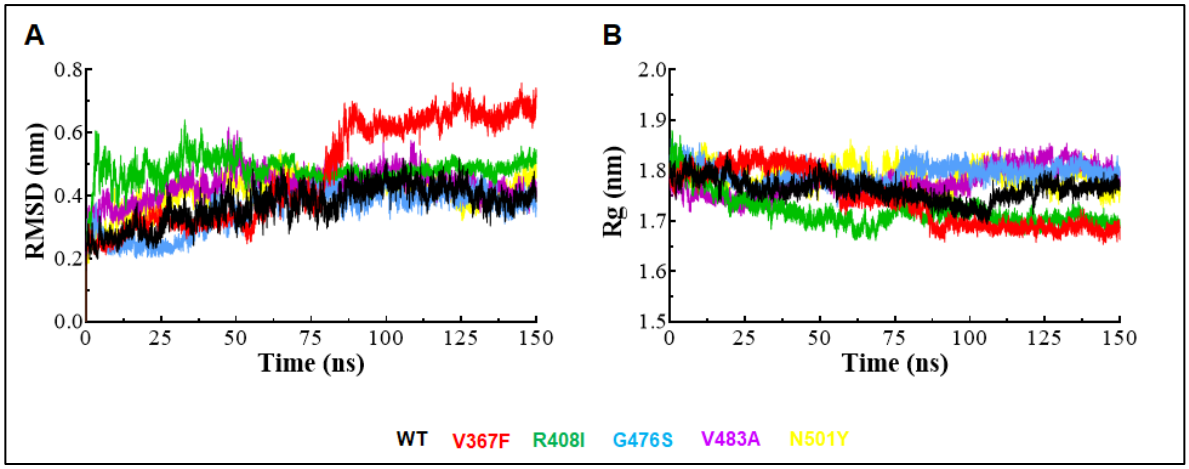

Fig. S2 **MD simulation profiles of WT and MT proteins.** (A) RMSD plot and (B) Rg plot. WT, V367F, R408I, G476S, V483A and N501Y MTs were labelled in black, red, green, blue, magenta and yellow colour, respectively.

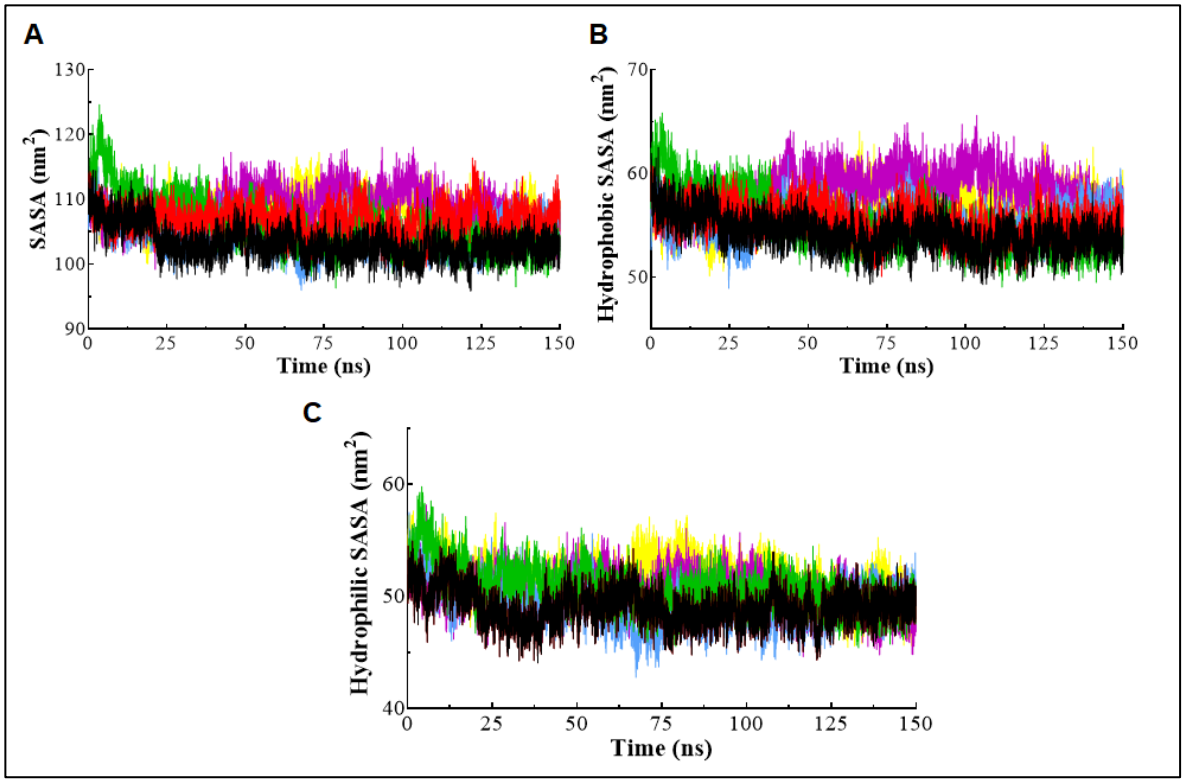

Fig. S3 **Solvent accessible surface area (SASA) analysis.** (A) Total SASA, (B) Hydrophobic SASA and (C) Hydrophilic SASA. WT, V367F, R408I, G476S, V483A and N501Y MTs were labelled in black, red, green, blue, magenta and yellow colour, respectively.

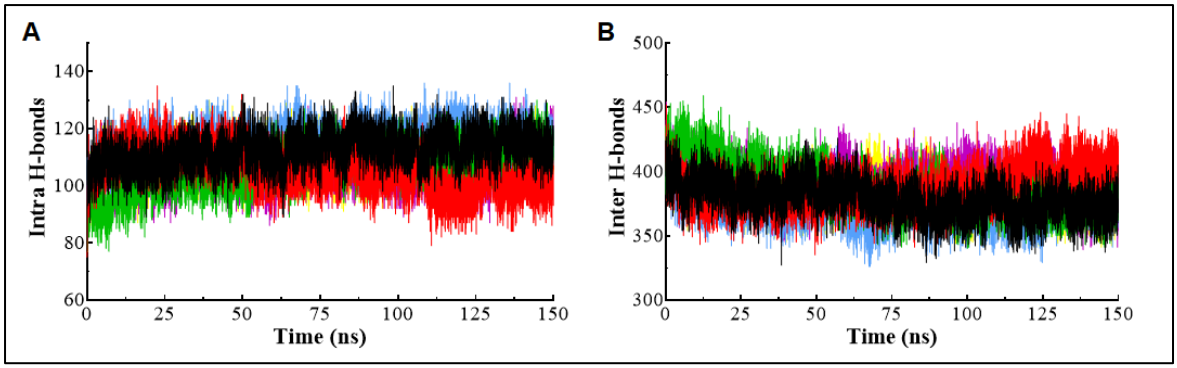

Fig. S4 **Hydrogen bond (H-bond) analysis.** (A) Intra or protein-protein H-bond and (B) Inter or protein-water H-bond. WT, V367F, R408I, G476S, V483A and N501Y MTs were labelled in black, red, green, blue, magenta and yellow colour, respectively.

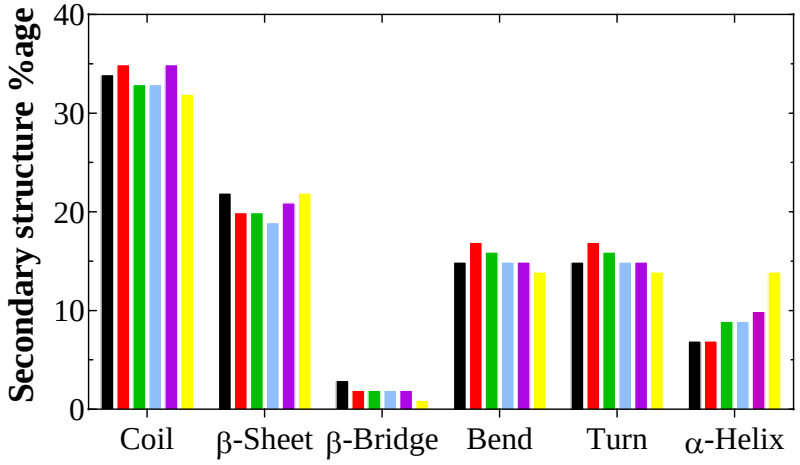

Fig. S5 **Secondary structure analysis of WT and MT proteins.** WT, V367F, R408I, G476S, V483A and N501Y MTs were labelled in black, red, green, blue, magenta and yellow colour, respectively.

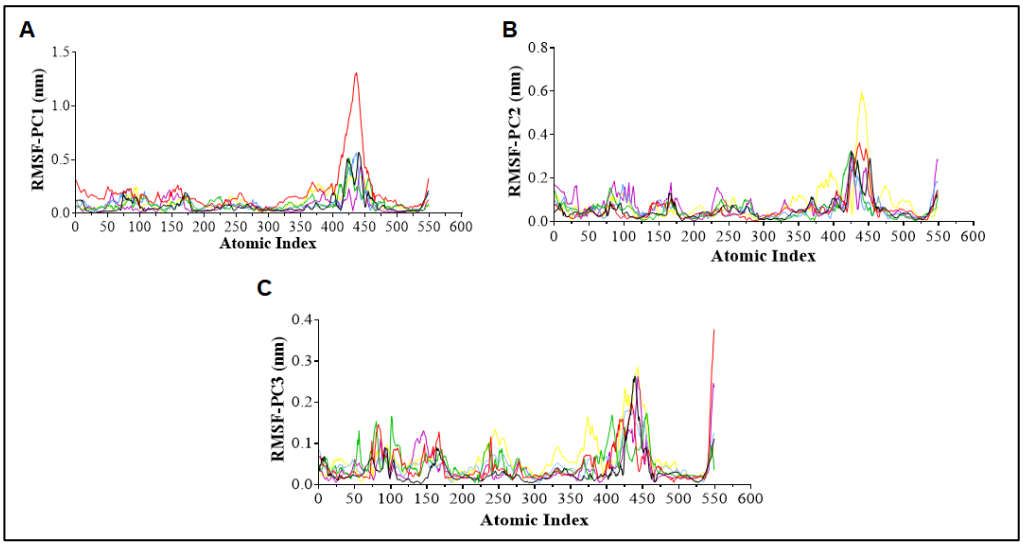

Fig. S6 **RMS fluctuation of first three PCs (PC1, PC2 and PC3) from WT and MTs.** WT, V367F, R408I, G476S, V483A and N501Y MTs were labelled in black, red, green, blue, magenta and yellow colour, respectively.

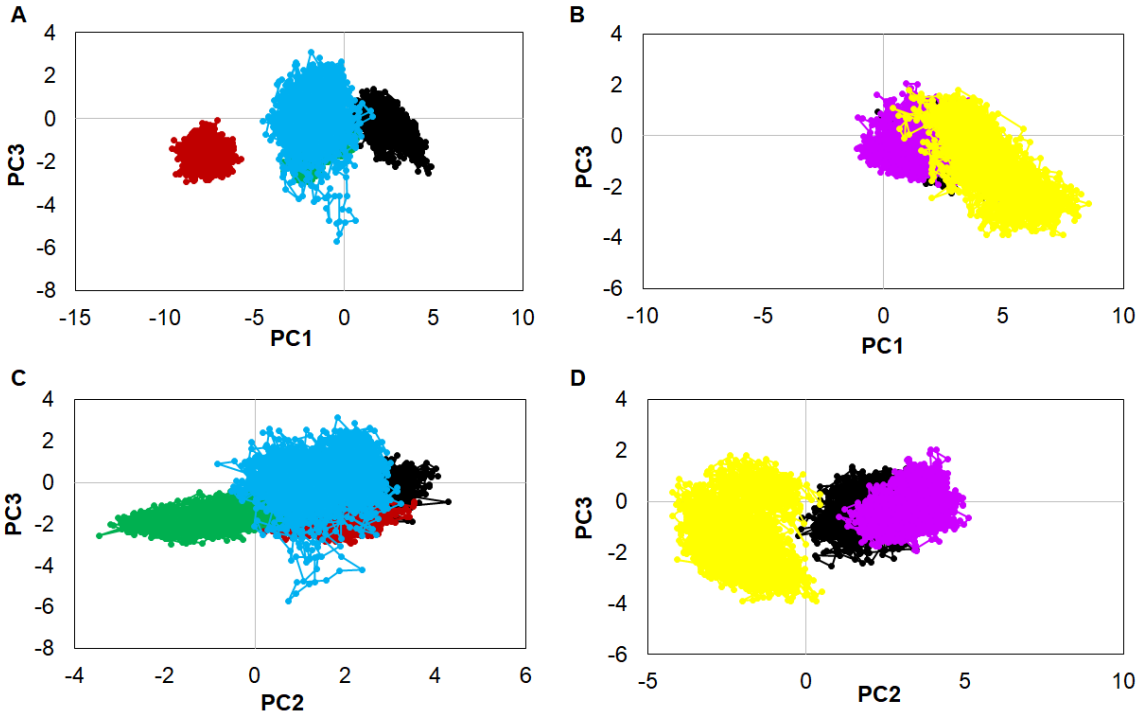

Fig. S7 Projection of eigenvector1 (PC1) vs eigenvector3 (PC3) and eigenvector2 (PC2) vs eigenvector3 (PC3). WT, V367F, R408I, G476S, V483A and N501Y MTs were labelled in black, red, green, blue, magenta and yellow colour, respectively.

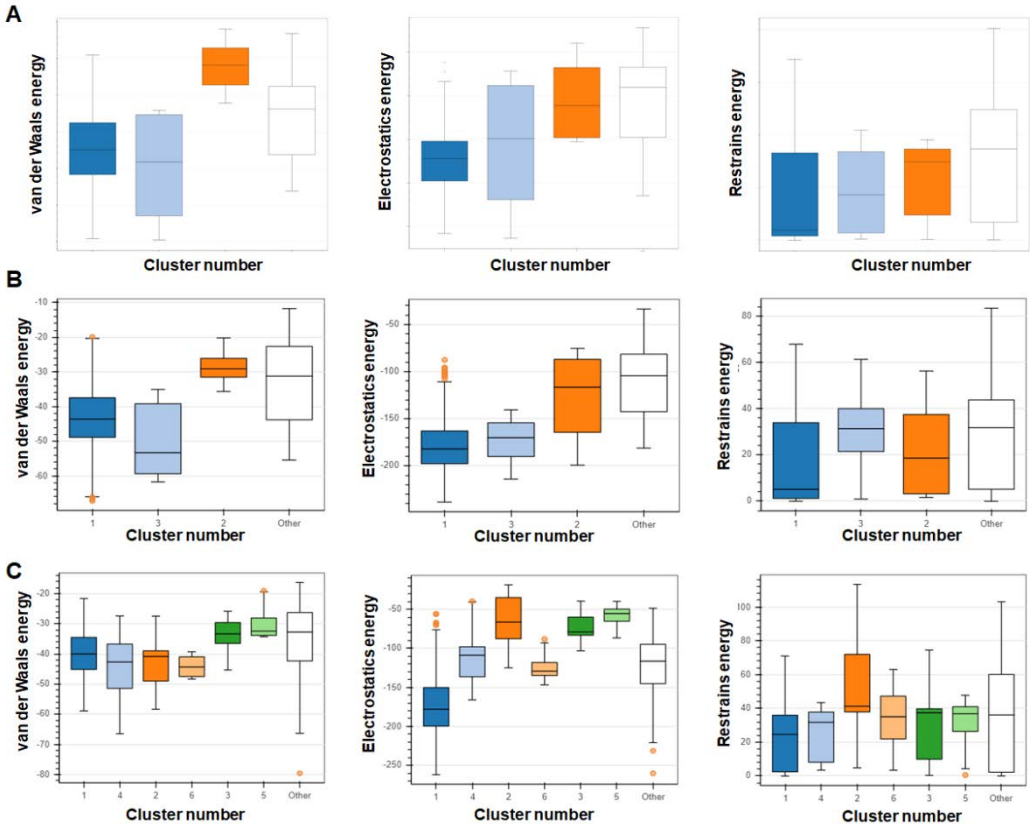

Fig. S8 Top clusters of protein-protein docking complexes. (A) ACE2-WT, (B) ACE2-V367F and (D) ACE2-R408I.

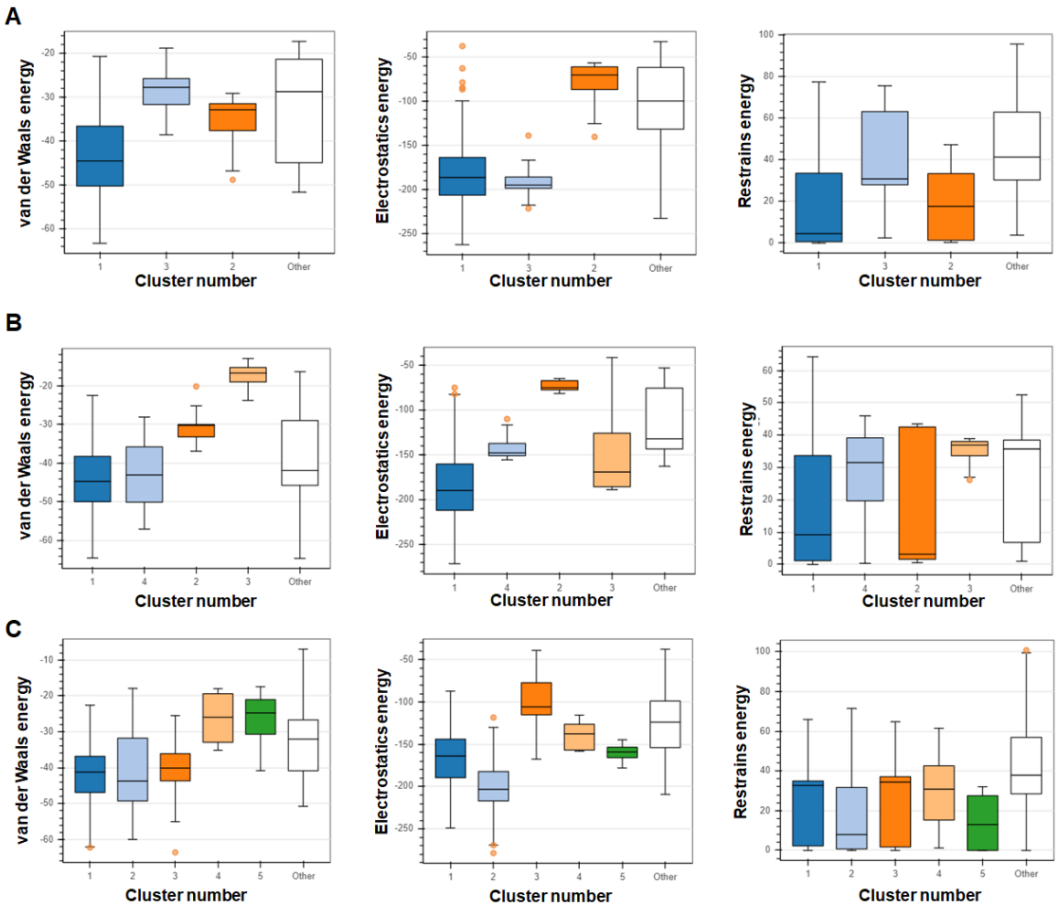

Fig. S9 Top clusters of protein-protein docking complexes contd. (A) ACE2-G476S, (B) ACE2-V483A and (C) ACE2-N501Y.

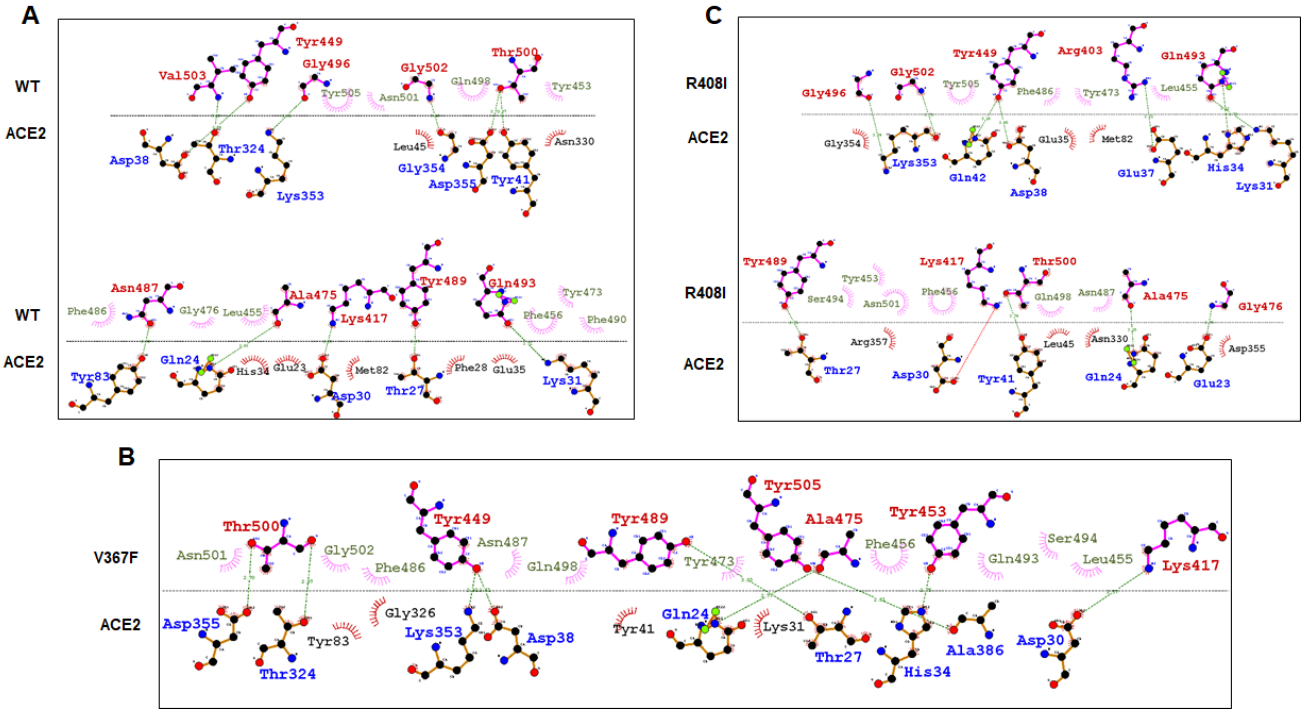

Fig. S10 2D interaction plots of (A) ACE2-WT (SpikeS1 RBD), (B) ACE2-V367F and (D) ACE2-R408I complexes. Hydrophobic and hydrophilic residues of ACE2 and SpikeS1 RBD were labelled in Black

(ACE2), light green (SpikeS1 RBD), blue (ACE2) and red (SpikeS1 RBD), respectively. Hydrogen bonds were labelled in green dotted lines.

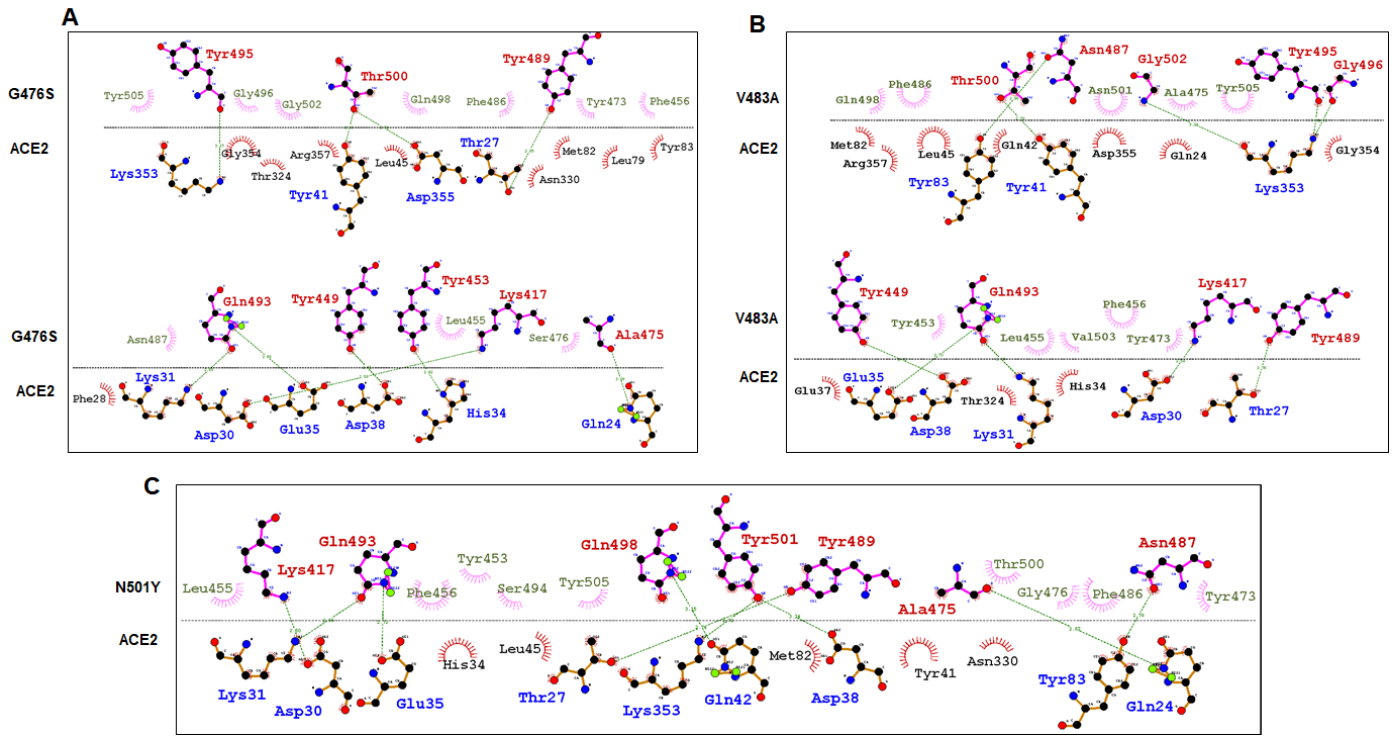

Fig. S11 2D interaction plots of (A) ACE2-G476S, (B) ACE2-V483A and (C) ACE2-N501Y complexes. Hydrophobic and hydrophilic residues of ACE2 and SpikeS1 RBD were labelled in black (ACE2), light green (SpikeS1 RBD), blue (ACE2) and red (SpikeS1 RBD), respectively. Hydrogen bonds were labelled in green dotted lines.

Table S1. Cumulative confirmed COVID-19 cases in million

Countries	January-June, 2020	July-December 2020	January, 2020 -September, 2021
USA	2.64	20.06	43.35
INDIA	0.58	10.27	33.74
BRAZIL	1.40	7.68	21.40

Table S2. Cumulative confirmed COVID-19 deaths per million

Countries	January-June, 2020	July-December, 2020	January, 2020 - September 2021
BRAZIL	266.69	911.0	2778.63
ITALY	575.02	1,226.54	1,603.89
USA	386.56	1,055.29	1,535.66

Table S3. Structure validation of different MT models along with WT

Variants	Favoured	Allowed	Disallowed	ProSA (Z-score)	QMEAN (Z-score)
WT	68.50%	29.50%	2%	-5.25	-7.94
V367F	68.50%	29.50%	2%	-5.27	-7.88
R408I	68.50%	29.50%	2%	-5.15	-8.15
G476S	68.50%	29.50%	2%	-5.23	-7.33
V483A	68.50%	29.50%	2%	-5.4	-7.95
N501Y	68.50%	29.50%	2%	-5.8	-7.99

Table S4. Protein stability prediction through MUpro server

		Support vector Machine		Neural Network		
Variants	**DDG**	**Stability**	**Confidence score**	**Stability**	**Confidence score**	**Stability**
V367F	-1.121	Decrease	-0.195	Decrease	-0.651	Decrease
R408I	0.497	Increase	0.007	Increase	-0.543	Increase
G476S	-0.715	Decrease	-0.45	Decrease	-0.566	Decrease
V483A	-1.175	Decrease	-0.505	Decrease	-0.999	Decrease
N501Y	-1.067	Decrease	0.391	Increase	0.790	Increase

Table S5. Protein stability prediction through I-Mutant server

Position	WT	New	Stability	DDG (Kcal/mol)
367	V	F	Decrease	-3.08
408	R	I	Decrease	-0.21
476	G	S	Decrease	-1.52
483	V	A	Decrease	-1.03
501	N	Y	Increase	0.15

Table S6. List of residues involved in hydrophobic and hydrophilic interactions during p-p docking.

	SpikeS1-RBD		ACE2	
Variants	**Hydrophilic**	**Hydrophobic**	**Hydrophilic**	**Hydrophobic**
WT	Lys417, Tyr449, Ala475, Asn487, Tyr489, Gln493, Gly496, Thr500, Gly502, Val503	Tyr453, Leu455, Phe456, Tyr473, Gly476, Phe486, Phe490, Gln498, Asn501, Tyr505,	Gln24, Thr27, Asp30, Lys31, Asp38, Tyr41, Tyr83, Thr324, Lys353, Gly354, Asp355,	Glu23, Phe28, His34, Glu35, Leu45, Met82, Asn330
V367F	Lys417, Tyr449, Tyr453, Ala475, Tyr489, Thr500, Tyr505,	Leu455, Phe456, Tyr473, Phe486, Asn487, Gln493, Ser494, Gln498, Asn501, Gly502,	Gln24, Thr27, Asp30, His34, Asp38, Thr324, Lys353, Asp355, Ala386,	Lys31, Tyr41, Tyr83, Gly326,
R408I	Arg403, Lys417, Tyr449, Ala475, Gly476, Tyr489, Gln493, Gly496, Thr500, Gly502,	Tyr453, Leu455, Phe456, Tyr473, Phe486, Asn487, Ser494, Gln498, Asn501, Tyr505,	Glu23, Gln24, Thr27, Asp30, Lys31, His34, Glu37, Asp38, Tyr41, Gln42, Lys353,	Glu35, Leu45, Met82, Asn330, Gly354, Asp355, Arg357,

G476S	Lys417, Tyr449, Tyr453, Ala475, Tyr489, Gln493, Tyr495, Thr500	Leu455, Phe456, Tyr473, Ser476, Phe486, Asn487, Gly496, Gln498, Gly502, Tyr505,	Gln24, Thr27, Asp30, Lys31, His34, Glu35, Asp38, Tyr41, Lys353, Asp355	Phe28, Leu45, Leu79, Met82, Tyr83, Asn330, Thr324, Gly354, Arg357
V483A	Lys417, Tyr449, Asn487, Tyr489, Gln493, Tyr495, Gly496, Thr500, Gly502	Tyr453, Leu455, Phe456, Tyr473, Ala475, Phe486, Gln498, Asn501, Val503, Tyr505,	Thr27, Asp30, Lys31, Glu35, Asp38, Tyr41, Tyr83, Lys353,	Gln24, His34, Glu37, Gln42, Leu45, Met82, Thr324, Gly354, Asp355, Arg357
N501Y	Lys417, Ala475, Asn487, Tyr489, Gln493, Gln498, Tyr501,	Tyr453, Leu455, Phe456, Tyr473, Gly476, Phe486, Ser494, Thr500, Tyr505,	Gln24, Thr27, Asp30, Lys31, Glu35, Asp38, Gln42, Tyr83, Lys353,	His34, Tyr41, Leu45, Met82, Asn330

Table S7. P-p interaction predicted by ClusPro server

ACE2-WT		ACE2-V367F		ACE2-R408I		ACE2-G476S		ACE2-V483A		ACE2-N501Y	
Cluster	Energy	Cluster	Energy	Cluster	Energy	Cluster	Energy	Cluster	Energy	Cluster	Energy
0	-942.4	0	-932.1	0	-937.3	0	-919.7	0	-924.7	0	-929.1
1	-851.9	1	-849.3	1	-838.6	1	-847.1	1	-858.3	1	-848.9
2	-781.6	2	-814.1	2	-775.5	2	-780.4	2	-780.1	2	-787.7
3	-781.9	3	-818	3	-792	3	-778.1	3	-787.3	3	-865.9
4	-869.1	4	-868	4	-870.3	4	-779.3	4	-760.2	4	-779.5
5	-773.9	5	-806.4	5	-794.1	5	-843.3	5	-854.2	5	-774.9
6	-811.9	6	-825.5	6	-773.9	6	-752.9	6	-787.7	6	-806.5
7	-773.5	7	-762	7	-814.6	7	-765.6	7	-777.8	7	-775.7
8	-884.8	8	-764.2	8	-835	8	-821.4	8	-776.8	8	-776.5
9	-779.8	9	-892.5	9	-904.6	9	-833.7	9	-811.1	9	-889.1
10	-900.2	10	-909.1	10	-782.8	10	-917.8	10	-741.3	10	-761.4
11	-848.8	11	-783.3	11	-759.4	11	-735.2	11	-770.3	11	-788.6
12	-806.7	12	-793.7	12	-814	12	-894.9	12	-734	12	-907.9
13	-762.1	13	-828.2	13	-765.5	13	-770.9	13	-778.7	13	-866
14	-807.9	14	-761.2	14	-790.8	14	-762.8	14	-854.5	14	-752.9
15	-774.2	15	-776.4	15	-788.4	15	-780.9	15	-803.5	15	-754.4
16	-746.3	16	-767	16	-743.7	16	-784.7	16	-837.8	16	-784.1
17	-776.5	17	-786.5	17	-773.7	17	-792	17	-847.8	17	-788.1
18	-738.1	18	-847.7	18	-762.8	18	-771.4	18	-761.3	18	-742.7
19	-787.1	19	-790.1	19	-872.7	19	-792.4	19	-793.8	19	-791.1
20	-786.8	20	-838.9	20	-737.1	20	-732.7	20	-784.6	20	-792.5
21	-765.4	21	-782.8	21	-785.6	21	-738.9	21	-789.5	21	-772.2
22	-720.2	22	-728.2	22	-718.8	22	-789.9	22	-785.4	22	-773.5
23	-840.2	23	-730.2	23	-748.8	23	-791.3	23	-727	23	-757.9
24	-751.7	24	-720.6	24	-814.4	24	-837.4	24	-737.8	24	-784.8
25	-787.8	25	-781.3	25	-784.9	25	-734.2	25	-718.2	25	-837.7
26	-712	26	-782.1	26	-836.2	26	-723.1	26	-779.6	26	-804.6
27	-778.9	27	-745.8	27	-789.7	27	-775.8	27	-759.4	27	-796.8
28	-732.3	28	-774.6	28	-731	28	-741.8	28	-694.5	28	-765.9
29	-784.7	29	-732.6	29	-724	29	-723.3	29	-727.8	29	-741.8

Table S8. P-p interactions predicted by pyDOCKWEB server

Complexes	Electrostatics energy (Elec)	Desolvation energy (Desolv)	Vander Waal energy (VDW)	Total energy (Elec+Desolv+0.1VDW)
ACE2-WT	-13.81	-26.45	42.59	-36.01
ACE2-V367F	-29.09	-16.14	-11.02	-46.33
ACE2-R408I	-12.52	-26.52	44.61	-34.58
ACE2-G476S	-14.06	-26.25	40.19	-36.30
ACE2-V483A	-22.30	-17.55	56.08	-34.25
ACE2-N501Y	-20.72	-19.06	-5.18	-40.30